Electronic structure and UPS of the misfit chalcogenide $(SnS)NbS_2$ and related compounds

E. E. KRASOVSKII[a], O. TIEDJE[a], W. SCHATTKE[a],

[a] Institut für Theoretische Physik und Astrophysik,
Christian-Albrechts-Universität, Leibnizstr. 15, 24098 Kiel, FRG

J. BRANDT[b], J. KANZOW[b], K. ROSSNAGEL, L. KIPP[b], M. SKIBOWSKI[b],

[b] Institut für Experimentelle und Angewandte Physik,
Christian-Albrechts-Universität, Leibnizstr. 19, 24098 Kiel, FRG

M. HYTHA[c], B. WINKLER[c],

[c] Mineralogisch-Petrographisches Institut,
Christian-Albrechts-Universität, Olshausenstr. 40, 24098 Kiel, FRG

Abstract

Based on the self-consistent band structure we present density-of-states (DOS) functions for a supercell structure $(SnS)_{1.2}NbS_2$ and discuss the intercalation effects. An *ab initio* UPS spectrum of $(SnS)NbS_2$ is compared to the experiment. The prototypes of the layer constituents of the misfit, PbS (NaCl) and $2H\text{-}NbS_2$ and $NbSe_2$, are studied; theoretical results are compared with available XPS and optical measurements. For PbS both relativistic effects and local field effects are found important. Experimental angle resolved UPS for $NbSe_2$ are compared to $\mathbf{k}_{||}$-projected DOS functions.

Keywords: Misfit; Photoemission; Optics

1 Introduction

Layered compounds with a mismatch of adjacent layers represent an interesting object to study interlayer chemical bonding. The structural investigations by traditional diffraction methods do not lead to results uniquely interpreted on a small length scale, thus the actual corrugation of the interface is not known exactly. For instance, the stress caused by the misfit of two neighboring lattice planes might be relaxed gradually on a mesoscale or periodically on a nanoscale through a displacement of interface atoms. The misfit $(SnS)NbS_2$ consists of a layered hexagonal transition metal dichalcogenide NbS_2 system, which has been regularly interdispersed by NaCl like layers of SnS into its van der Waals gaps [1]. The misfit occurs along one layer parallel lattice direction, say a, whereas b matches for both subsystems. Existing bandstructure calculations explain main features of the chemical bonding in the misfits [2]. The apparent stability of the system, i.e. the interlayer attraction, is assumed to originate from charge transfer between the layers, though definite quantitative data are still to be expected from electronic structure calculations.

Owing to the presence of a van der Waals gap, an *ab initio* simulation of the layer distortion by a straightforward geometry optimization is not possible: the state-of-the-art computational schemes based on the local density approximation or generalized gradient approximations of the density functional theory fail to describe the long range interaction between the layers. [3]

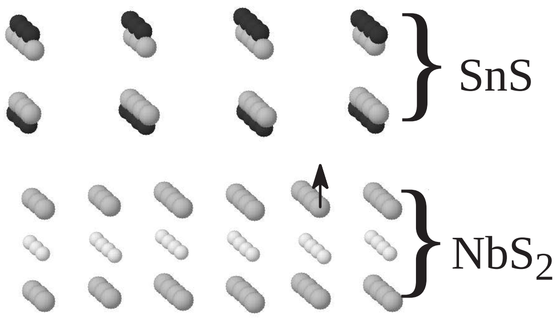

Figure 1: Monoclinic unit cell of $(SnS)_{1.2}NbS_2$. Two calculations are performed: for the ideal NbS_2 layer and with a displacement of the sulphur atom (shown by arrow).

As an attempt to use spectroscopic information to get insight into the properties of misfits we have calculated ultraviolet photoelectron spectra of $(SnS)NbS_2$ on the basis of self-consistent bulk band structure. To minimize possible ambiguities resulting from the chosen supercell geometry as well as from our simplified theoretical model of photoemission (namely the neglect of surface effects and the use of Kohn-Sham eigenvalues for quasi-particle energies) we also study spectral properties of related crystals, NbS_2, $NbSe_2$, and PbS (no valence band spectroscopy data are available for NaCl-type SnS).

2 Computational technique

We present supercell calculations for a system with the composition formula $(SnS)_{1.2}NbS_2$ built of alternate double layers of SnS and sandwiches of NbS_2 (Fig.1). The composition is fixed by a matching forced on a length of 5 unit cells of NbS_2 along the a direction and three unit cells of SnS, the actual composition being $(SnS)_{1.17}NbS_2$.

The calculations are performed with the extended linear augmented plane wave **kp** method (ELAPW-**kp**). The **kp** formalism [4] reduces the **k**-point dependence of the APW basis set to a multiplication of the APWs with a reference Bloch vector $\mathbf{k}_0$ by the function $\exp[i(\mathbf{k}-\mathbf{k}_0)\mathbf{r}]$. Thus, the time-consuming operations of setting up the hamiltonian, overlap, and momentum matrices are performed only once for a given crystal potential. The computer time for these procedures scales as n^3 with the number of atoms in the unit cell. (The hamiltonian matrix dimension is ~ 2000.) On the other hand, the Brillouin zone (BZ) shrinks and the number of **k**-points to be considered reduces. An accurate self-consistent crystal potential for the misfit can be constructed by interpolating between only three irreducible points in the BZ. However, to obtain reliable spectroscopic information it is necessary to perform the integrations over the **k**-space with a higher accuracy and, consequently, to take into account a large number of **k**-points. This makes the **kp** method an indispensable tool for such calculations. We found the tetrahedron method for UPS to converge with 14 irreducible points (48 inequivalent tetrahedra).

To check the stability of our results to peculiarities of the computational scheme we also performed *ab initio* pseudopotential calculations [5] for $(SnS)NbS_2$ and NbS_2.

3 Results and discussion

The **X-ray photoemission** spectrum for $(SnS)NbS_2$ for $\hbar\omega = 1486.6$ eV [2] is compared with the calculated DOS function in Fig. 2. The width of the valence band (VB) and the location of experimentally resolved structures is well reproduced. As in the pure hexagonal chalcogenides NbS_2 or $NbSe_2$ the NbS_2 layer of the misfit gives rise to five maxima in the upper VB. The sulphur atoms of the SnS sublayer contribute to the main maximum at $E - E_F = -2$ eV. In contrast to the misfit, in the experimental XPS spectrum of $NbSe_2$ [7] the five maxima are well resolved (see the lowermost panel of Fig. 2 (a)).

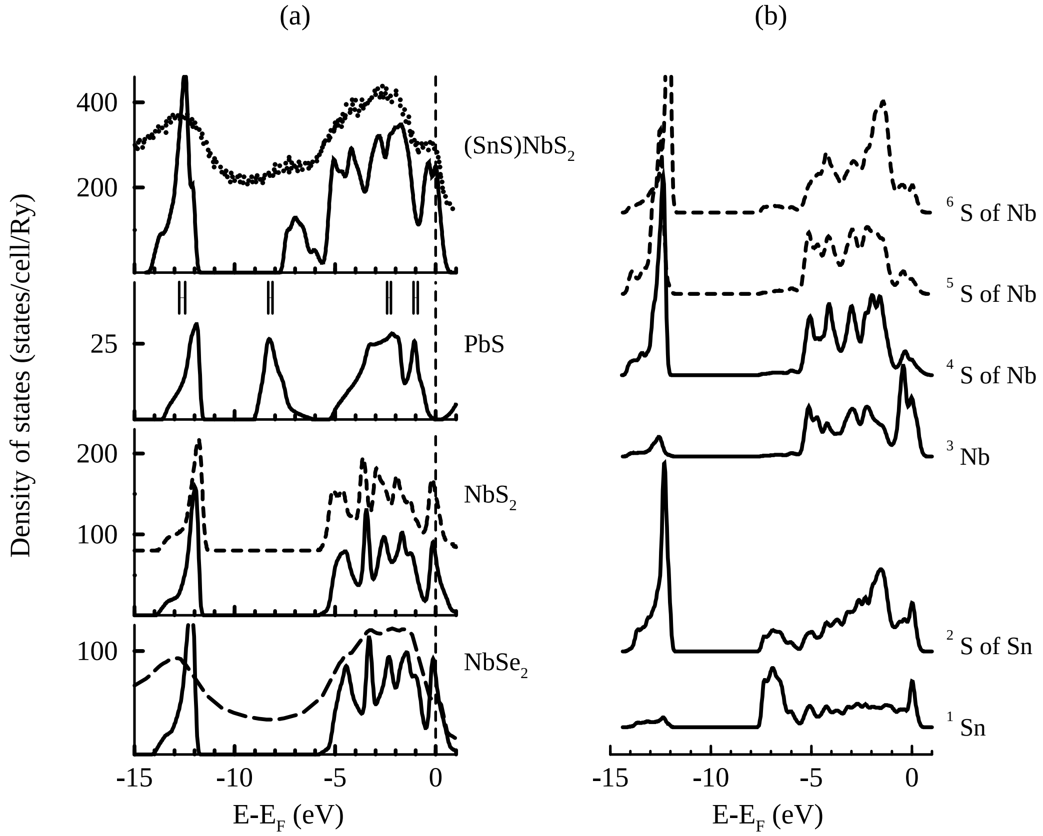

Figure 2: (a) Density of states for $(SnS)NbS_2$ and related crystals. $(SnS)NbS_2$: dots show XPS data of Fang et al. [2], DOS is for the case of a distorted NbS_2 sandwich. PbS: bars mark relative energy locations and experimental uncertainties of the maxima in the XPS spectrum of McFeely et al. [6]. The marks are shifted by 0.2 eV to higher energies to place the Pb 6s peak to its calculated position at -8.3 eV. NbS_2: DOS by the ELAPW-**kp** method (lower curve) is compared to that by an *ab initio* pseudo-potential method [5]. $NbSe_2$: Dotted curve shows XPS data by Wertheim et al. [7]. (b) Atom-resolved partial DOS for $(SnS)NbS_2$. The curves 1 to 4 are for the case of ideal NbS_2 sublattice. Crystallografically inequivalent sites of Nb, Sn, or S produce essentially the same DOS, so function of a single representative site is shown. Curves 5 and 6 are for a distorted NbS_2 sandwich; curve 5 shows an in-plane S atom, and curve 6 the displaced atom.

The smearing of the structures in the misfit compound can be explained by the corrugation of the NbS_2 sublayer. We have performed calculations for two geometries: in the first case we have chosen the NbS_2 layer to be identical to that in pure 2H-NbS_2 (ideal sandwich), and in the second case the sandwich is distorted by shifting one of five inequivalent sulphur atoms by 0.2 Å from the $z = const$ plane in the z direction towards the SnS sublattice (see Fig. 1). We have found the displacement to cause a considerable broadening of all the maxima in the total DOS curve. The changes in the DOS on the sulphur sites of the NbS_2 layer are illustrated in Fig. 2 (b).

For example, both maxima around -2 eV in the sulphur DOS of the ideal NbS_2 sandwich (curve 4) are well resolved, whereas they merge into each other when the sandwich is distorted (curve 5). The minima between peaks flatten as one proceeds from curve 4 via 5 to 6. Furthermore, the displacement of the sulphur atom enhances the -1.5 eV maximum in the DOS of this atom by about 100%. Here, the comparison stresses that a considerable nonuniform deviation from the ideal crystal structure, apart from the incommensurability, must be present in the considered sample. In addition, the similarity is striking between the the sulphur DOS curve of the SnS layer (curve 2) and that of the displaced atom (curve 6) with respect to both the -1.5 eV peak and the peak at the Fermi edge. The displaced sulphur atom strongly hybridizes with the SnS sulphur receiving also electron density from the SnS layer.

For the **UV photoemission** spectra we have used the model of direct transitions between bulk states. Theoretical energy distribution curves for (SnS)NbS_2 for three photon energies are compared in Fig. 3 with the measured UPS [2] for 21.2 eV. The momentum conservation constraint makes the structures in the UPS much sharper than in the DOS curve. The dipole selection rules suppress the intensity of Sn 5*s* emission and enhance the emission from the bottom of NbS_2 band (around -5 to -4 eV). These trends are confirmed by the experiment.

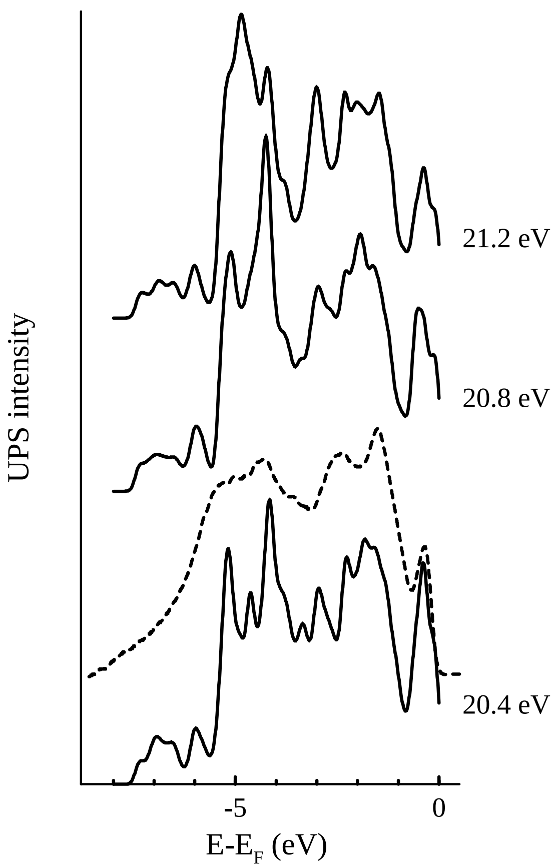

Figure 3: Ultraviolet photoemission spectra of (SnS)NbS_2. Dashed curve shows the experiment of Ref. [2] for $\hbar\omega = 21.2$ eV. Full curves show calculated energy distribution curves for $\hbar\omega = 20.4$, 20.8, and 21.2 eV.

However, the fine structure between -2.5 and -1.5 eV does not agree with that of the measured spectrum: a sharp minimum at -2.5 eV is present in the calculated spectra for all photon energies around 21.2 eV and we never observe a maximum at that energy. At small binding energies the shape of the spectrum is determined by the structure of initial states: the minimum at -2.5 and maximum at -3 eV are present in the DOS curve. We have found this fine structure sensitive to approximations to the crystal potential: in the pseudopotential calculation the minimum and the maximum are located ~0.2 eV lower in energy than in the all-electron calculation. The uncertainty is, however, still too small to be considered a reason for the discrepancy with the experiment. The experimentally observed fine structure may arise from the corrugation of the sulphur layer of the NbS_2 sandwich. The local DOS on the displaced sulphur atom shows a much weaker minimum at -2.5 eV (curve 6 in Fig. 2 (b)) and the intensity is transferred to the region around -1.5 eV.

Focusing on the structure between -5 and -3.5 eV one can see the experimental spectrum to compare better with theoretical spectra for photon energies lower than 21.2 eV. Such a slight shift of the theoretical final states' energy scale may be produced by a non-zero real part of the self-energy.

Independent information about unoccupied states is provided by optical measurements. In Fig. 4 we compare calculated **reflectivity** of PbS to the measured spectrum [8]. To our knowledge, this is the first calculation that takes into account both the effects of spin-orbit coupling and the local field effects. The technique we use to calculate the full dielectric matrix is presented in Ref. [10]. The relativistic effects are seen to be strong over the whole energy range; at low frequencies they are due to the splitting of unoccupied Pb $6p$ states and in the far UV range the splitting of semi-core $5d$ states is important. The inclusion of local field effects improves the absolute values of the far UV reflectivity but does not change the shape of the spectrum. All structures in the theoretical spectrum are shifted by 0.45 eV to lower energies with respect to their measured positions, which is a typical failure of the one-electron theory based on Kohn-Sham electron states. A discrepancy of the same order of magnitude we have observed for the **loss function** of $NbSe_2$ in the far UV region: our calculations predict the strong plasmon peak at 20.6 eV, whereas in the experiment [9] it is found at 21 eV. Thus, the value between 0.4 and 0.8 eV we have assumed for the self-energy shift in the UPS of $(SnS)NbS_2$ appears to be realistic.

In theoretical simulation of the angular integrated UPS it is very difficult to take into account surface effects. On the other hand, angular resolved UPS measurements (ARUPS), which could provide information about the dispersion of the bands in the surface region, are not available for the $(SnS)NbS_2$ misfit. To reveal the difference between the electronic structure of the NbS_2 terminated crystal surface and the bulk we present in Fig. 5 our measured dispersion of the peaks in the ARUPS of 2H-$NbSe_2$ for $\hbar\omega = 21.2$ eV with the $\mathbf{k}_{||}$ changing along the ΓM line and compare it to theoretical 1D DOS functions for irreducible $\mathbf{k}_\perp$ lines parallel to the ΓA direction, and $\mathbf{k}_{||}$ scanning the ΓM interval. The use of a different anion (Se) for reasons of sample preparation seems to be of minor importance.

The localized Nb $4d$ states are not strongly affected by the surface effects; in the UPS of $(SnS)NbS_2$, Fig. 3, the Nb $4d$ states give rise to the peak at -0.4 eV (-0.3 eV in the experiment). In $NbSe_2$, Fig. 5, the measured $\mathbf{k}_{||}$ onset of the Nb $4d$ emission peak just below the Fermi level agrees with the theoretical prediction: the structure becomes visible for $k_{||} > 0.45\Gamma$M.

The dispersion of the bottom of the $\mathbf{k}_{||}$ projected VB reproduces that of the lowermost experimental peak: its minimal binding energy (the narrowest VB) is observed at $k_{||} = 0.55\Gamma$M. For $k_{||} < 0.3\Gamma$M the peak at the VB bottom is well resolved and the structure is seen to be shifted rightwards by ~ 0.4 eV. For larger $k_{||}$ the experimental structure

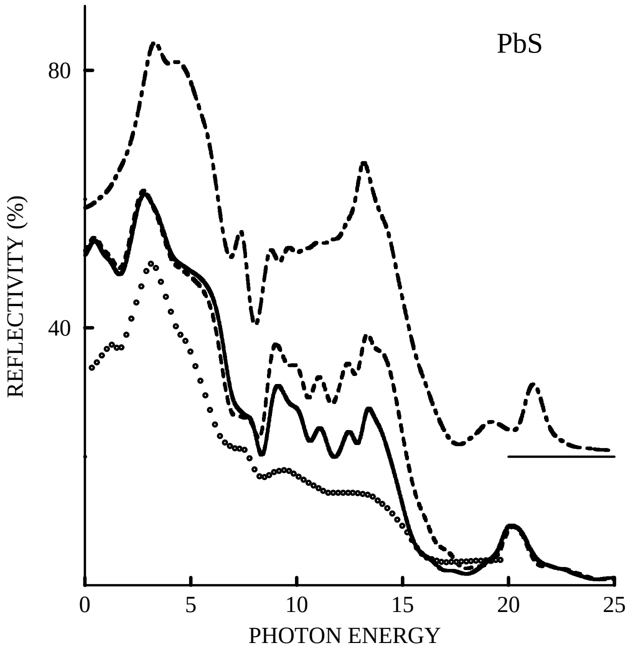

Figure 4: Optical reflectivity of PbS; dot-dashed curve shows a scalar-relativistic calculation without local fields, lower curves show relativistic calculations with (full) and without (dashed) local fields. Experiment (dots) is by Cardona and Greenaway [8]; the curve is shifted by 0.45 eV to the right.

becomes much weaker, and close to point M it is well visible again and it is located ~ 0.2 eV lower than in the theory. The discrepancies at the VB bottom reveal the changes in the electronic structure in the surface region, however, the surface effects are apparently strongly $\mathbf{k}_{||}$ dependent and are blurred in the angular integrated photoemission. Indeed, the UPS measurements of $NbSe_2$ by Shepherd and Williams [11] show the VB bottom at the same energy as in XPS [7] and in the DOS curve.

In the experimental ARUPS we observe a weakening of emission around $E - E_F \sim -3$ eV between $k_{||} = 0.5$ and 0.85ΓM (an empty elliptic spot in the left panel), which is in contrast to the appreciable DOS in this region. This disagreement might be due to matrix elements' or final states' effects and it correlates with the broader experimental minimum at that binding energy in the UPS of (SnS)NbS_2 (Fig. 3). Matrix elements have been included in the theoretical curves of Fig. 3, however, the discrepancy might result from our using bulk instead of true scattering states as final states.

The above comparison of the site-resolved DOS (Fig. 2), UPS (Fig. 3), and ARUPS (Fig. 5) reveal the dominance of the NbS_2 layer in the photoemission of the misfit and supports our assumption that the uppermost layer of the misfit is the NbS_2 layer.

4 Conclusions

In spite of the lack of important crystallographic information our model calculations of the XPS and UPS spectra of the misfit compound (SnS)NbS_2 reproduce experimental data with a good quality. We conclude that the photoemission properties of (SnS)NbS_2 mainly reflect the electronic structure of the NbS_2 layer, which, in turn, depends upon the interaction with the SnS layer via the displacements of sulphur atoms. The corrugation of the NbS_2 sandwich manifests itself most vividly in the binding energy range around -1.5 eV.

The conduction band states have appeared to be a plausible approximation for the

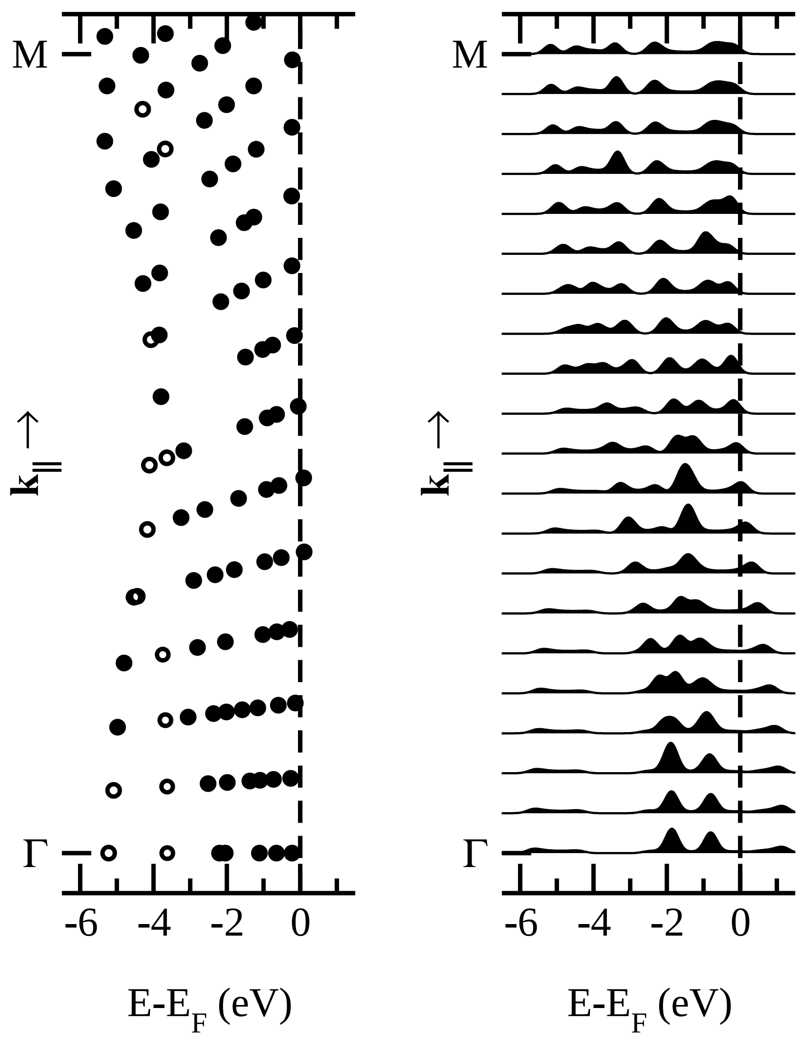

Figure 5: Peak dispersion in the UPS of $NbSe_2$ taken along the ΓM direction at $\hbar\omega =$ 21.22 eV. Dots in the left panel denote peaks obtained by fitting the spectra by a sum of Voigt profiles convoluted with the experimental resolution function. In the right panel the 1D $\mathbf{k}_{||} = const$ DOS functions are shown, with $\mathbf{k}_{||}$ changing from ΓA to ML.

photoemission final states; the comparison with the experiment and the study of the optical properties of PbS and $NbSe_2$ suggest that the self-energy effects are moderate and can be taken into account by a uniform shift of the final states' energies by ~ 0.5 eV.

Two characteristic features in the angular resolved UPS measurements of $NbSe_2$ can be directly related to those of $\mathbf{k}_{||}$-projected bulk band structure, namely, the dispersion of the Nb $4d$ peak near the Fermi energy and the dispersion of the bottom of the valence band. The features that have a transparent bandstructure origin are important for a further investigation of dichalcogenide layers in complex compounds, where full photoemission theory is computationally forbidding.

Acknowledgment

Work supported by the Deutsche Forschungsgemeinschaft, Forschergruppe DE 412/21.

References

[1] Y. Ohno, Phys. Rev. B, 44 (1990) 1281.

[2] C.M. Fang, A.R.H.F. Ettema, C. Haas, G.A. Wiegers, H. van Leuken and R.A. de Groot, Phys. Rev. B, 52 (1995) 2336.

[3] W. Kohn, Y. Meir and D.E. Makarov, Phys. Rev. Lett., 80 (1998) 4153.

[4] E.E. Krasovskii and W. Schattke, Phys. Rev. B, 56 (1997) 12874.

[5] CASTEP User Guide. Molecular Simulations Inc., San Diego, CA, 1998.

[6] F.R. McFeely, S. Kowalczyk, L. Ley, R.A. Pollak and D.A. Shirley, Phys. Rev. B, 7 (1973) 5228.

[7] G.K. Wertheim, F.J. DiSalvo and D.N.E. Buchanan, Solid State Commun. 13 (1973) 1225.

[8] M. Cardona and D.L. Greenaway, Phys. Rev., 133 (1964) A1685.

[9] M.G. Bell and W.Y. Liang, Adv. Phys., 25 (1976) 53.

[10] E.E. Krasovskii and W. Schattke, Phys. Rev. B, 60 (1999) 16251.

[11] F.R. Shepherd and P.M. Williams J. Phys. C: Solid State Phys., 7 (1974) 4427.